

LASER INTERFEROMETER GRAVITATIONAL WAVE OBSERVATORY
- LIGO -
CALIFORNIA INSTITUTE OF TECHNOLOGY
MASSACHUSETTS INSTITUTE OF TECHNOLOGY

Proceeding LIGO-P960041-02 - R Dec. 20, 96
Recent Research on the LIGO 40 m Interferometer
Seiji Kawamura

This is a proceeding
for the TAMA conference (1996).

California Institute of Technology
LIGO Project - MS 51-33
Pasadena CA 91125
Phone (818) 395-2129
Fax (818) 304-9834
E-mail: info@ligo.caltech.edu

Massachusetts Institute of Technology
LIGO Project - MS 20B-145
Cambridge, MA 01239
Phone (617) 253-4824
Fax (617) 253-7014
E-mail: info@ligo.mit.edu

WWW: <http://www.ligo.caltech.edu/>

Recent Research on the LIGO 40 m Interferometer

Seiji KAWAMURA for the LIGO Project

California Institute of Technology, M/S 51-33, Pasadena, California 91125

ABSTRACT

The LIGO (Laser Interferometer Gravitational-Wave Observatory) 40m interferometer at Caltech has recently made two major advances which were necessary milestones to ensure the LIGO interferometer design: incorporating the recombination configuration and testing a new suspension system. The 40m recombined optical configuration was the first operation of a suspended-mass Fabry Perot interferometer in which signals carried by the optically recombined beams were used to detect and control all the important test mass displacements. The experimental results were found to be in generally good agreement with the theoretical analysis of the performance expected from such an interferometer. A prototype of the new suspension system, which has the same basic design as the planned LIGO suspension, was also installed and characterized in the 40m interferometer for locking performance and sensitivity. The features and performance of the new suspension design were found to be desirable for the LIGO suspension.

1 Introduction

The Laser Interferometer Gravitational-Wave Observatory (LIGO) Project [1] is developing facilities aimed at detecting and studying gravitational waves from astrophysical sources. The LIGO detectors will use highly sensitive laser interferometry to measure the relative motions of four test masses placed at the ends of two perpendicular 4 km long arms. One of the principal research tools used in this effort is the 40 meter interferometer [2] at Caltech. It is used to test many of the features of the planned 4 km long detectors. The 40m interferometer has recently made two major advances which were necessary milestones to ensure the LIGO interferometer design: incorporating the recombination configuration [3] and testing a new suspension system. [4] This report discusses these two advances and also the future work in the 40 m interferometer.

2 Recombined Interferometer¹

2.1. Motivation and Significance

The optical topology chosen for the initial LIGO interferometer is a power recycled Michelson with Fabry-Perot arm cavities with the asymmetry signal extraction scheme. The 40 m interferometer had been operated as a locked Fabry-Perot interferometer since its original commissioning until 1995. In this configuration, as shown in Fig. 1, the light returning from the

1. This work was carried out by Torrey Lyons and the LIGO team.

two arms was independently sensed by two photodiodes. The frequency of the light was stabilized with the first arm as a reference, and the second arm length was measured using this stabilized light. The modification of the 40 m interferometer to a recombined optical topology using the asymmetry signal extraction scheme is, therefore, a necessary intermediate step toward the full recycled optical topology in the 40 m interferometer.

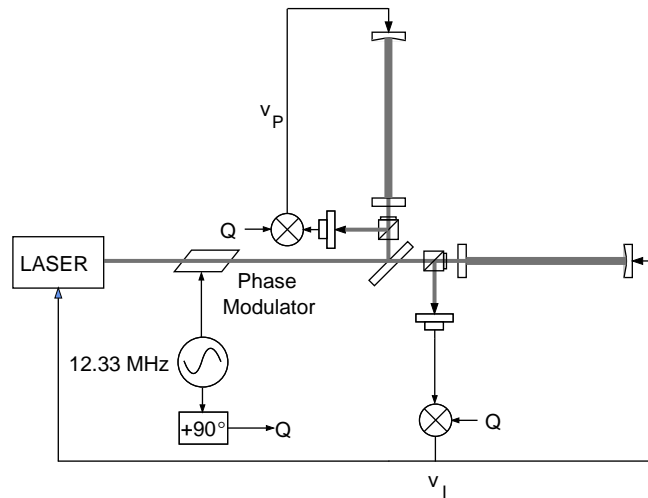


Fig. 1 Locked Fabry-Perot optical and control topology.

2.2. System Description

A diagram of the recombined optical and control topology with asymmetric scheme is shown in Fig. 2. The recombined beam at the symmetric port is demodulated with the in-phase modulating signal (I) or the quadrature-phase signal (Q) and produces signals, v_1 or v_2 , respectively. The recombined beam at the anti-symmetric port is demodulated with the quadrature-phase signal and produces a signal, v_3 . This scheme is valid due to the asymmetry in the Michelson arm lengths. The signal, v_1 is used to control the frequency of the light to the common mode arm cavity length. The signal, v_2 is fed back to the beam splitter control system to control the differential Michelson

length. The signal, v_3 is used to control the differential arm cavity length. All three signals depend primarily on the degree of freedom they control.

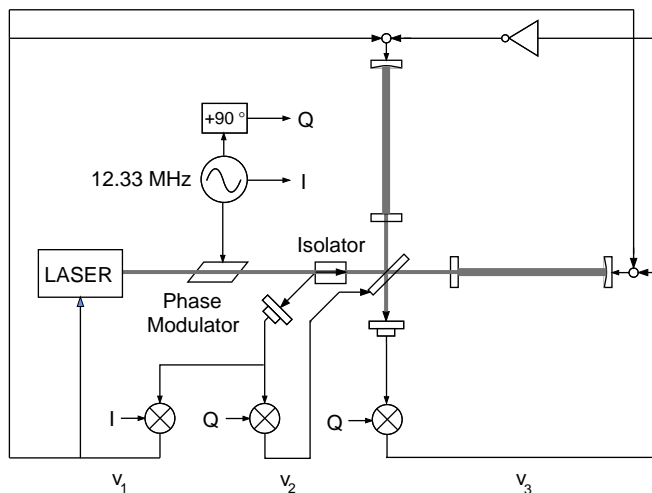


Fig. 2 Recombined optical and control topology.

2.3. Performance

2.3.1. Sensitivity

Figure 3 shows the sensitivity of the 40 m interferometer with the recombined configuration together with the predicted shot noise curves. The shot noise was estimated by two methods: calculation and empirical measurement. The shot noise was calculated using the measured parameters such as modulation depth, reflectivity and transmission of the mirror (See Table 1). The empirical measurement of the shot noise was accomplished by blocking the laser light and shining incandescent light on the antisymmetric photodiode. The interferometer readout signal was then calibrated with the effect of the loop gain properly accounted for. The calculated shot noise agrees with the empirical measurement within the uncertainties of the parameters in the calculation. The effect of shot noise on the symmetric photodiode was verified to be negligible by both theory and experiment. However, the interferometer sensitivity does not seem to be limited by shot noise at any frequency, although the frequency dependence of the interferometer noise above 500 Hz is very similar to that of shot noise. This discrepancy was confirmed to be true by attenuating the light at the antisymmetric port and observing much smaller degradation in noise than expected if the sensitivity were limited by shot noise. All the known noise sources were carefully estimated,

but nothing explained the noise above 500 Hz. This is one outstanding unresolved issue in the recombined interferometer experiment.

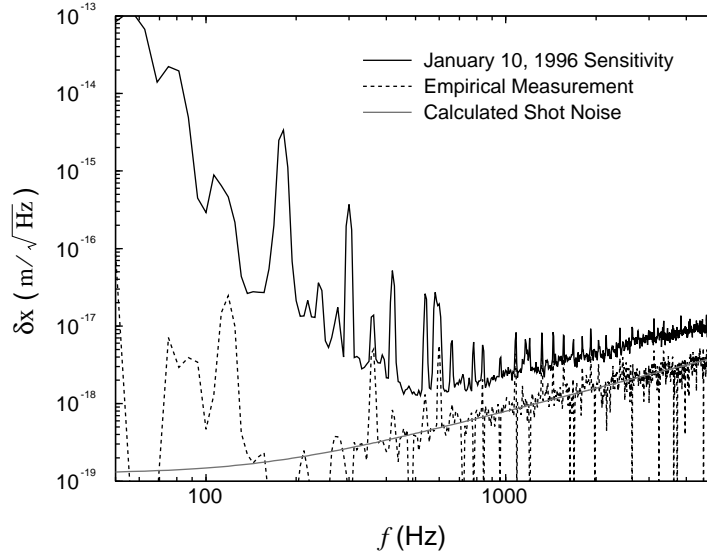


Fig. 3 Sensitivity of the recombined interferometer with the predicted shot noise.

Table 1: Optical parameters for the recombined interferometer.

Quantity		Value
Transmission	Beamsplitter	0.45
	Input mirror	280 - 300 ppm
	End mirror	12 ppm
Loss	Input mirror	110 ppm
	End mirror	56 ppm
Asymmetry		50.8 cm
Modulation frequency		12.33 MHz
Modulation index		0.7 - 1.49
Contrast defect, $1 - C$		0.03

2.3.2. Lock Acquisition

The largest concern before the operation of the recombined interferometer was the undefined mechanism for the lock acquisition. The fundamental problem is that the Fabry-Perot cavities using RF reflection locking techniques only provide a signal which is linearly proportional to their length for very small deviations from resonance. It is even more difficult in a suspended interfer-

ometer with high finesse. The lock acquisition sequence observed was that the beam splitter acquired lock first because of its broad range of linear operation, and then the common mode control system acquired lock to hold one of the arm cavities on resonance, and finally the remaining arm was locked by the differential mode control system after a while. It was a surprise that the resonance of the arm brought by the common mode control system was not disrupted by the intermittent chirp which was a contribution of the out-of-lock arm while it was passing through resonances. This sequence was similar to the situation we had with the locked Fabry-Perot interferometer.

2.3.3. Phase reversal

A problem with the lock acquisition sequence is that the signal to control the beamsplitter reverses sign in going from the case of one arm and the beamsplitter in lock to the entire interferometer in lock. This is because the overcoupled Fabry-perot arm cavities switch the phase of the reflected carrier light by 180° going from out of lock to in lock, as shown in Fig. 4. A practical method to avoid this problem is to increase the modulation depth, which changes the sign of the beamsplitter error signal for the all-lock state with the sign maintained for the one-arm-lock state. Table 2 shows that increasing the modulation depth changes the v_2 signal on the differential Michelson phase ϕ_- , whereas the other diagonal components, the signal v_1 on the common mode arm cavity phase Φ_+ and v_3 on the differential mode arm cavity phase Φ_- , are not affected at all. This is due to a beating between the first and second order sidebands, neither of which experience a phase reversal when the arm cavities go into resonance. This method worked reliably and it didn't degrade the sensitivity of the 40 m interferometer, because it was not limited by the shot noise. Another method we tried was to incorporate an automatic switch of the polarity change of the beamsplitter control system triggered by the locking of the both arm cavities. This system also worked, although not as reliably as the other method.

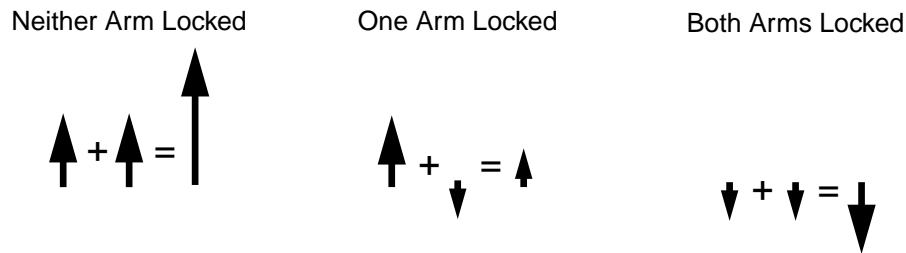


Fig. 4 Phaser diagram of the reflected carrier light to the symmetric port.

Table 2: Extracted signal sensitivity at different modulation depth.

Phase	∂v_1		∂v_2		∂v_3	
	0.7	1.49	0.7	1.49	0.7	1.49
$\partial\Phi_+$	-7.8	-7.8	0	0	-2.2×10^{-1}	-2.2×10^{-1}
$\partial\phi_-$	2.3×10^{-4}	2.3×10^{-4}	-1.3×10^{-5}	1.9×10^{-4}	-1.0×10^{-5}	-1.9×10^{-4}
$\partial\Phi_-$	2.5	2.5	-2.5×10^{-9}	1.6×10^{-8}	1.0	1.0

3 New Suspension System¹

3.1. Motivation and Significance

The suspension system is one of the essential subsystem of the LIGO interferometer. The main function of the suspension system is to isolate a test mass from ground motion, to damp the motion of the test mass, and to provide inputs for length and alignment control signal. The design effort of the LIGO suspension started with establishing the requirements of the suspension system in 1995. Meanwhile the 40 m interferometer had been using the suspension system of the first generation since the 40m interferometer was born. In 1991 the control system of the suspension was replaced to improve the sensitivity of the interferometer drastically at low frequencies, but the mechanical system still remained the same. We had found many undesirable features on this first-generation suspension system, and finally in 1993 a new suspension system of the second generation was designed for the small optics, such as the beam splitter and the mode cleaner mirrors. This type of the suspension system was adopted for the phase noise interferometer in MIT, too. Since then, we have found some unsatisfactory features on this system when we closely looked at the system, considering the requirements for the LIGO suspension. In 1995 we designed the suspension system of the third generation to demonstrate concepts of the LIGO suspension design; this third-generation suspension system has all the improvement incorporated based on our experience and the LIGO requirements.

3.2. System Description

The schematic view of the mechanical system and the control system of the 40 m test mass suspension is shown in Fig.5 and Fig. 6, respectively. The test mass is suspended by a single loop suspension wire from the suspension block on the top plate of the suspension support structure. The wire standoffs and the guide rods are used to balance the test mass. Six magnet/standoff assemblies are glued to the test mass and five sensor/actuator heads are mounted on the head holders. The suspension support structure is strengthened by the stiffening bars. The test mass is pro-

1. This work was carried out by Seiji Kawamura and the LIGO team.

ected by the safety cage and the safety bar which contain the safety stops. The position and angle of the test mass are detected by the edge sensor which consist of a pair of LED and photodiode. Either this signal or a signal from the 40m optical lever sensor is filtered, amplified and fed back to the coil to damp the test mass motion. A bias signal and an interferometer length control signal are injected in the control loop.

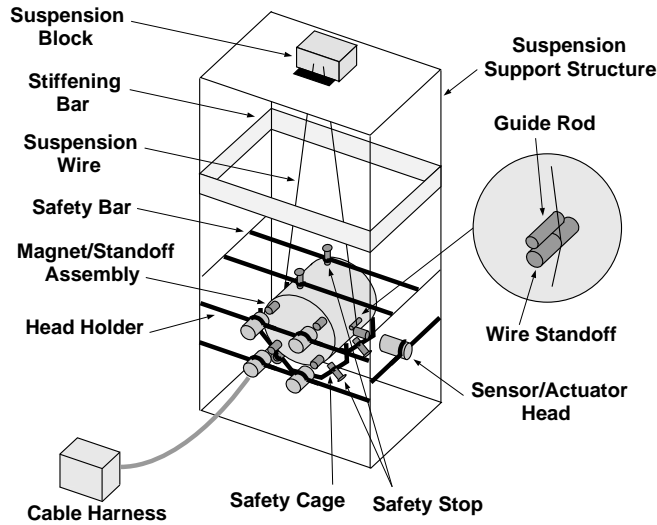


Fig. 5 Schematic view of the mechanical system of the 40 m test mass suspension.

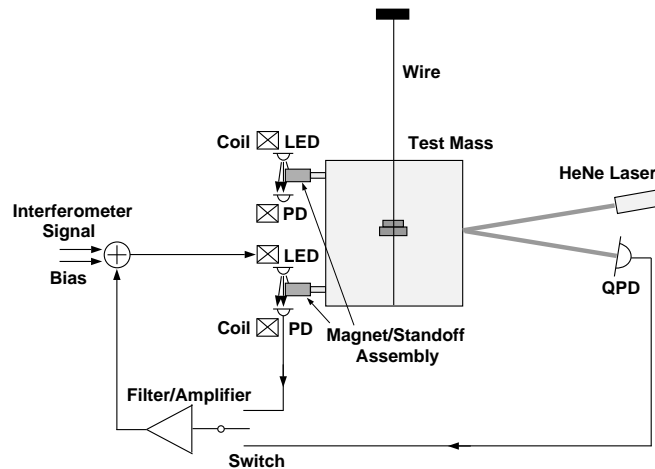


Fig. 6 Schematic diagram of the control system of the 40 m test mass suspension.

3.3. Performance

3.3.1. Single Loop Wire

The new suspension system employs a single loop wire instead of double loops. The single loop wire scheme simplifies the mechanical design of the suspension significantly. It is, thus, less

subject to practical thermal losses due to complicated mechanics which may cause undesirable thermal noise in some modes. The single loop suspension is also free from any high-frequency resonances which arose from the complicated mechanism of the double loop wire suspension. The first-generation suspension system used a control block from which the test mass was suspended by two loops of wire. Figure 7 shows the schematic view of the old suspension. This system had a pitch resonance frequency of around 100 Hz above which the test mass and the control block moves in pitch with anti-phase. The Q factor of the pitch resonance was measured to be 2,000 - 3,000, from which the thermal noise of this pitch mode was predicted to be close to the noise spectrum of the interferometer around 100 Hz. Figure 8 shows the displacement sensitivity of the 40 m interferometer as of Oct. 28, 94 together with the predicted noise of various sources. It can be seen that at least two noise peaks at 80 Hz and 110 Hz are very likely due to the pitch thermal noise.

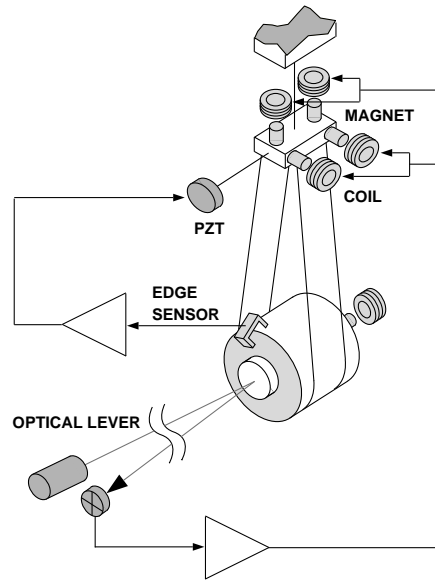


Fig. 7 Schematic view of the old 40m test mass suspension.

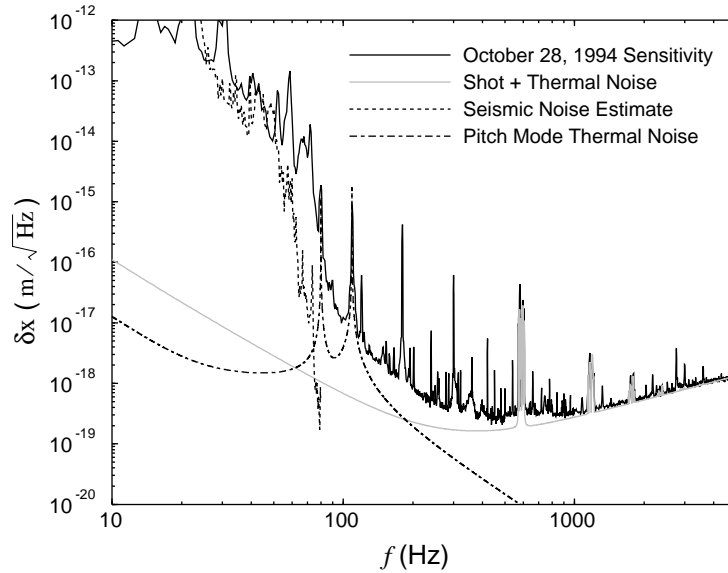


Fig. 8 Displacement sensitivity of the 40m interferometer and noise prediction of various sources.

Since only one of the four old suspensions was replaced with the new suspension this time, we could not observe any significant improvement around 100 Hz in the noise spectrum after the replacement. However, it is expected that replacement of the remaining old suspensions with the new suspensions in near future will improve the noise performance around 100 Hz.

It was a concern that balancing the test mass in pitch might be difficult using only one loop of wire. As shown in Fig. 9, guide rods and wire standoffs were used to balance the test mass. A small aluminum guide rod was first glued to the mass. A larger aluminum rod was then placed below the guide rod between the test mass and the wire. The wire standoff has a groove on it, on which the wire rests. The test mass was balanced in pitch adjusting the position of the wire standoff along the guide rod using a piezoelectric buzzer. This procedure allowed balancing the test mass in pitch within 0.5 mrad from the vertical direction dictated by gravity.

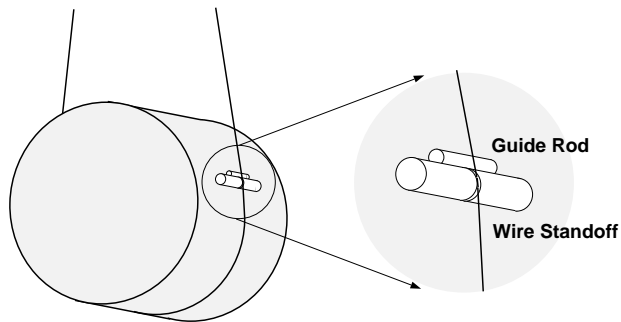


Fig. 9 Guide rod and wire standoff.

3.3.2. Edge Sensor without Vane

The new suspension system employs a simple edge sensor without vane. As shown in Fig. 10, an LED and photodiode pair senses the shadow of the magnet. The magnet does not have any vane on it; the magnet itself acts as a vane. This design ensures minimum degradation of the thermal noise of the test mass internal mode due to additional attachments to the mass. This “no vane” scheme is also good to keep the resonance frequency of the magnet/standoff assembly high.

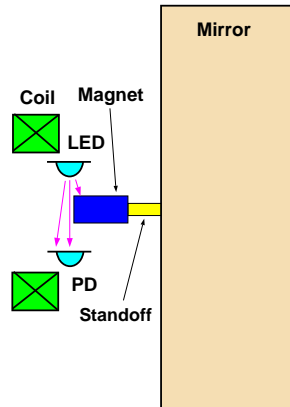


Fig. 10 Edge sensor without a vane in the new suspension system.

The second-generation suspension system used a slot sensor instead of an edge sensor. Figure 11 shows the slot sensor with a big vane with a slot through which the LED light shines the split photodiode. The differential signal of the split photodiode gives the position signal of the test mass. The essential point behind this design is that the LED intensity can be stabilized using the sum output of the split photodiode. However, it requires the vane to be too large, which is not only bad for thermal noise of the test mass internal mode but also undesirable in terms of mechanical features. The resonance frequency of the vane/magnet/standoff assembly was found to be as low as 1 kHz, which could interfere with a control system with a unity gain frequency of around 1 kHz.

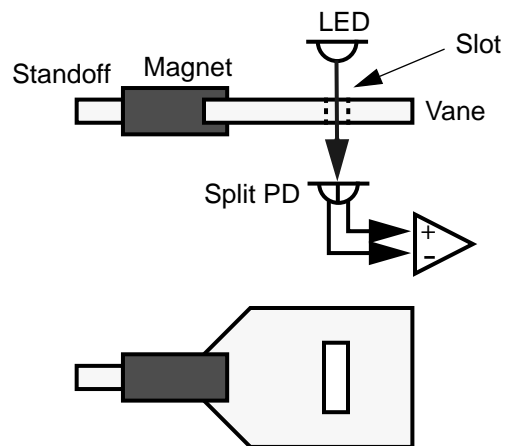


Fig. 11 Slot sensor and a large vane in the second-generation suspension system.

We measured the lowest resonance frequency of the magnet/standoff assembly without a vane to be 7.7 kHz; this is high enough not to interfere with the control system. The biggest concern of this design was that large cross-coupling of sensing between each degree of freedom due to no vane might cause instability in the control system. It turned out that by carefully aligning the relative position of the magnet to the sensor within 500 μm or so, the control system can be made stable and robust. Another concern was the stability of the sensor; no active intensity stabilization is available for the edge sensor. It was found that the stability of the LED power was well below the shot noise level of the sensor above 50 Hz, when the current to the LED was passively stabilized.

4 Future Work

4.1. Recycling¹

The program to convert the 40 m interferometer to a recycled configuration has started recently (summer in 1996). The vertex masses have already been replaced with ones of higher transmission. Reconfiguration of the vacuum envelope to accommodate the recycling mirror is underway. The recycled interferometer will provide exciting opportunities to answer questions which are to be solved before the LIGO design is finalized. Understanding the lock acquisition process in the recycled configuration is necessary to proceed to the LIGO interferometer. A suspended recycled interferometer will also provide the chance to investigate noise performance with the same configuration as LIGO.

4.2. Beamsplitter Suspension²

The prototype of the suspension system for the LIGO small optics, such as the mode cleaner mirrors, has already been built. It will be tested as the beamsplitter suspension in the 40 m interferometer. The installation of the new beamsplitter suspension will take place during the reconfiguration of the vacuum envelope for the recycled interferometer. This system has a mechanical design similar to the second-generation suspension with features of the new 40m test mass suspension. It has a VME-based control system, so that the gain, matrix coefficient, and polarity switch, etc. are all controlled on the computer screen instead of by turning knobs.

5 Summary

The 40m recombined optical configuration was the first operation of a suspended-mass Fabry Perot interferometer in which signals carried by the optically recombined beams were used to detect and control all the important test mass displacements. The experimental results were found to be in generally good agreement with the theoretical analysis of the performance expected from such an interferometer. The lock acquisition was found to be quite easier than expected. The phase reversal of the beamsplitter control signal, which had not appreciated before the experiment, was coped with cleverly. The experiment of the recycled interferometer has been started, and will provide useful information for the LIGO design.

1. This work is being carried out by Jennifer Logan and the LIGO team.
2. This work is being carried out by Seiji Kawamura and the LIGO team.

A prototype of the new suspension system, which has the same basic design as the planned LIGO suspension, was also installed and characterized in the 40m interferometer for locking performance and sensitivity. The features and performance of the new suspension design, such as a single loop wire and simple edge sensor, were found to be desirable for the LIGO suspension. The prototype of the LIGO small optics suspension will be installed and tested as a beamsplitter suspension in the 40 m interferometer. This will give useful feedback to finalize the LIGO small optics suspension.

Acknowledgments

I thank the entire LIGO team, because this work was done by the LIGO team led by Barry Barish. Torrey Lyons was the main contributor for the recombination work, and Jenny Logan is a task leader for the recycling experiment. This work was supported by the National Science Foundation cooperative agreement number PHY-9210038.

References

- [1] A. Abramovici, W. E. Althouse, R. W. P. Drever, Y. Gursel, S. Kawamura, F. J. Raab, D. Shoemaker, L. Sievers, R. E. Spero, K. S. Thorne, R. E. Vogt, R. Weiss, S. E. Whitcomb, M. E. Zucker, *Science* **256**, (1992) p.325
- [2] A. Abramovici, W. Althouse, J. Camp, D. Durance, J. Giaime, S. Kawamura, A. Kuhnert, T. Lyons, F. Raab, R. Savage, D. Shoemaker, L. Sievers, R. Spero, R. Vogt, R. Weiss, S. Whitcomb, and M. Zucker, *Phys. Lett.* **A218** (1996) p.157
- [3] T. Lyons, Ph.D thesis, California Institute of Technology (1996)
- [4] S. Kawamura, J. Hazel, and J. Heefner, LIGO Internal Working Note, LIGO-T960162-02-D (1996)